Accepted for oral presentation at the Optical Society of America's
Propagation Through and Characterization of Atmospheric and Oceanic Phenomena,
26 - 29 June 2017, San Francisco, CA.

Observations of microscale internal gravity waves over an orchard canopy

Shane D. Mayor
California State University, Chico
400 West First Street, Chico, CA 95929, USA.
sdmayor@csuchico.edu

Abstract: Scanning atmospheric lidar and in situ observations of internal gravity waves with wavelengths ranging from 30 m to 100 m in the atmospheric roughness sublayer over a forest canopy will be presented.

OCIS codes: 010.3640 (lidar), 010.3920 (meteorology), 010.1330 (atmospheric turbulence)

1. Introduction and Background

This paper is a summary of a manuscript that has been submitted by the author to *Agricultural and Forest Meteorology* and is in peer review at the time of this writing.

Temperature inversions routinely form during the night over land when the surface of the earth cools faster than the air above it. Such environments are statically stable arrangements of the lowest levels of the atmosphere that resist the production of turbulence and support vertical oscillations known as internal gravity waves [1–4]. This paper presents observations of organized groups of internal gravity waves in the very stable, nocturnal atmospheric boundary layer over a $(1.6\ \text{km})^2$ walnut orchard block in central California. The dataset is unique because of the simultaneous availability of wind velocity and air temperature measurements from mast-mounted fast-response in situ sensors in the form of time-series at multiple altitudes, and 2D images of relative aerosol backscatter from a ground-based scanning elastic lidar system. Use of both types of data begin to reveal the 3D structure and motion of waves in the atmospheric roughness sublayer. The waves are significant because if they continue to amplify they will eventually result in unstable vertical arrangements of the air that lead to *breaking* and episodes of turbulence that are responsible for vertical fluxes of heat, momentum, and trace gases [5]. Their characteristics may also be of interest to those studying the propagation of horizontally directed laser radiation very close to the surface of the earth.

Waves over forest canopies are commonly referred to as *canopy waves* because they result from the shear-induced inflection point instability [6] that the canopy induces on the mean horizontal flow. Prior studies of canopy waves include those by [7–20]. The waves described herein likely correspond to the waves shown in panels a and b of Fig. 14 in [16]. That is, most of them appear to have a sinusoidal shape in the direction of the mean flow such as Fig. 14a in [16] and about 42% of the cases exhibit an asymmetry in the horizontal wave structure that is characteristic of Kelvin-Helmholtz billows such as Fig. 14b in [16]. These phases of wave development occur prior to the more developed turbulence that makes it difficult to recognize the turbulent coherent structures that occur after the waves break such as Figs. 14c and 14d in [16].

2. Experiment and Methodology

The data was collected during the Canopy Horizontal Array Turbulence Study (CHATS) [21]. The Raman-shifted Eye-safe Aerosol Lidar (REAL) [22–24] was located 1.44 km north of the northern edge of the orchard. A 30-m tall instrumented tower was installed in the orchard at 1.61 km range from the REAL. The lidar and the in situ sensors operated continuously between March and June of 2007. After the experiment the time-lapse animations of the nearly-horizontal PPI scans were carefully examined for the presence of fine-scale wave packets [25]. 53 wave episodes were identified from the 3-month data set. Episodes range in time from a few minutes to more than 1 hour in duration. To focus the analyses and extract the salient features of the environment supporting the wave activity, a 5-minute period of time per episode corresponding to when the waves appeared most pronounced in the lidar imagery was chosen. The lidar imagery provides several important quantities that cannot be obtained from the in situ data: wavelength and wave propagation velocity (speed and direction).

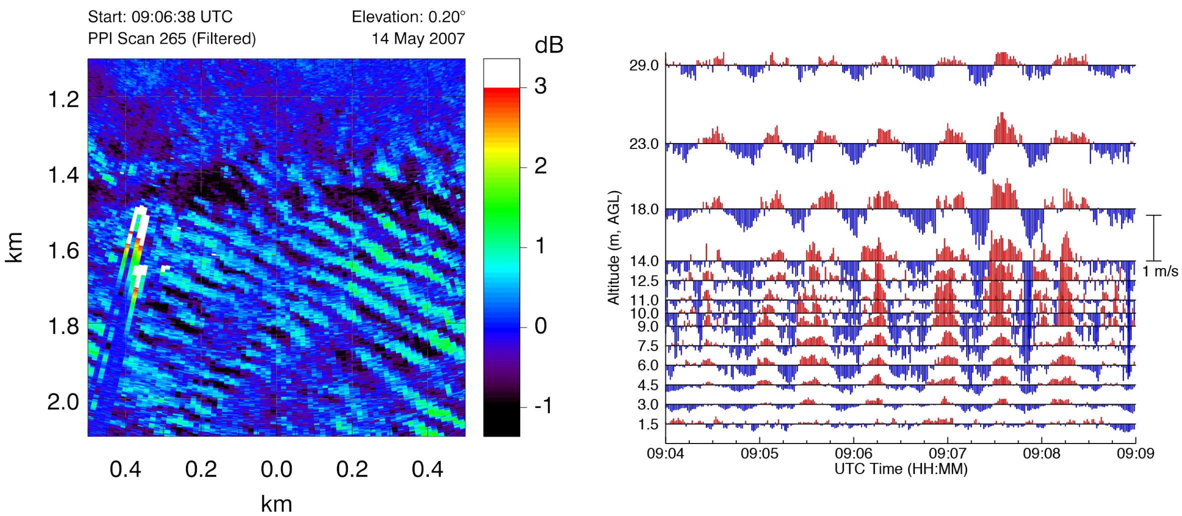

Fig. 1. Example of data from one canopy wave episode. Left: Numerically filtered elastic backscatter intensity in a 1 km by 1 km horizontal cross-section at about 18 m AGL through the waves on 14 May 2007 at 09:06:38 UTC. Right: Time series of vertical velocity from 13 sonic anemometers at altitudes ranging from 1.5 to 29 m AGL. The tower supporting the in situ sensors was located in the center of the image on the left.

3. Key Findings and Conclusions

All wave episodes occurred during the night when temperature inversions, strong static stability, and light winds were present. Vertical profiles of mean horizontal wind speed, shear, and concavity reveal a maximum in shear at the canopy top. Moreover, a change in the sign of concavity and the existence of an inflection point in the mean wind profiles exists. The values of concavity below 10 m AGL tend to be positive and the values of concavity above 10 m AGL tend to be negative. The in situ data was also used to compute the gradient Richardson number (*Ri*) for each of the 53 episodes. The *Ri* profiles show considerable scatter above and below the canopy height of 10 m, but are strongly clustered between 0 and 0.15 in the range of altitudes between 8 m and 13 m AGL. This cluster of values at the canopy top is less than the critical *Ri* of 0.25, indicating that this region is dynamically unstable and prone to the generation of instability resulting in waves or turbulence. These observations are consistent with the prevailing theory that the waves are due to the drag that the canopy induces on the flow and the resulting inflection point instability.

Perhaps the most novel finding is that the waves propagate in the same direction as the wind but at phase speeds less than the mean wind speed. Furthermore, very careful inspection of the lidar imagery reveals that the wave crests in 22 of the 53 cases are asymmetric. Specifically, the upwind side of the wave crests exhibit a sharper horizontal gradient of aerosol backscatter while the downwind sides are more diffuse. This observation is consistent with the notion that the flow is more laminar on the upwind side and turbulent on the downwind edge as the waves begin to break and mix any previous stratification of the aerosol. These observations are consistent with observations of Kelvin-Helmholtz billows elsewhere. A correlation between the mean environmental conditions and the wavelengths was not found.

Now that the canopy wave episodes have been cataloged, and the salient characteristics of the waves and supporting environments documented, it is possible to continue research by examining the microscale structure of the waves. Such details may be of more interest to the pcAOP community since it should be possible to use the in situ data to compute gradients of refractive index through the wave train.

Acknowledgements This work was supported by NSF AGS 0924407 and 1228464.

References

1. H. J. S. Fernando and J. C. Weil, "Whither the stable boundary layer?" Bull. Amer. Meteor. Soc. **91**, 1475–1484 (2010).
2. B. R. Sutherland, *Internal Gravity Waves* (Cambridge University Press, Cambridge, UK, 2010).
3. C. J. Nappo, *An Introduction to Atmospheric Gravity Waves* (Academic Press, Oxford, UK, 2012).
4. L. Mahrt, "Stably stratified atmospheric boundary layers," Annual Review of Fluid Mechanics **46**, 23–45 (2014).
5. J. Sun, C. J. Nappo, L. Mahrt, D. Belusic, B. Grisogono, D. R. Stauffer, M. Pulido, C. Staquet, Q. Jiang, A. Pouquet, C. Yague, B. Galperin, R. B. Smith, J. J. Finnigan, S. D. Mayor, G. Svensson, A. A. Grachev, and W. D. Neff, "Review of wave-turbulence interactions in the stable atmospheric boundary layer," Reviews of Geophysics **53**, 956–993 (2015). 2015RG000487.
6. P. K. Kundu, I. M. Cohen, and D. R. Dowling, *Fluid Mechanics* (Academic Press, Oxford, UK, 2016), sixth ed.
7. D. R. Fitzjarrald and K. E. Moore, "Mechanisms of nocturnal exchange between the rain forest and the atmosphere," J. Geophys. Res **95(D10)**, 16,839–16,850 (1990).
8. K. T. Paw U, Y. Brunet, S. Collineau, R. H. Shaw, T. Maitani, J. Qiu, and L. Hipps, "On coherent structures in turbulence above and within agricultural plant canopies," Ag. and Forest Met. **61**, 55–68 (1992).
9. M. R. Raupach, J. J. Finnigan, and Y. Brunet, "Coherent eddies and turbulence in vegetation canopies: the mixing-layer analogy," Bound. Layer Meteor. **78**, 351–382 (1996).
10. X. Lee, T. Black, G. den Hartog, H. H. Neumann, Z. Nesic, and J. Olejnik, "Carbon dioxide exchange and nocturnal processes over a mixed deciduous forest," Ag. and Forest Met. **81**, 13–29 (1996).
11. X. Lee, "Gravity waves in a forest: A linear analysis," J. Atmos. Sci. **54**, 2574–2585 (1997).
12. X. Lee, H. H. Neumann, G. D. Hartog, J. D. Fuentes, T. A. Black, R. E. Mickle, P. C. Yang, and P. D. Blanken, "Observation of gravity waves in a boreal forest," Bound. Layer Meteor. **84**, 383–398 (1997).
13. X. Lee and A. G. Barr, "Climatology of gravity waves in a forest," Quart. J. R. Met. Soc. **124**, 1403–1419 (1998).
14. M. Pulido and G. Chimonas, "Forest canopy waves: the long-wavelength component," Bound. Layer Meteor. **100**, 209–224 (2001).
15. X. Hu, X. Lee, D. E. Stevens, and R. B. Smith, "A numerical study of nocturnal wavelike motion in forests," Boundary-Layer Meteorology **102**, 199–223 (2002).
16. J. J. Finnigan, R. H. Shaw, and E. G. Patton, "Turbulence structure above a vegetation canopy," J. Fluid Mech. **637**, 387–424 (2009).
17. K. Gavrilov, G. Accary, D. Morvan, D. Lyubimov, S. Méradji, and O. Bessonov, "Numerical simulation of coherent structures over plant canopy," Flow, Turbulence and Combustion **86**, 89–111 (2011).
18. S. E. Belcher, I. N. Harman, and J. J. Finnigan, "The wind in the willows: flows in forest canopies in complex terrain," Annu. Rev. Fluid Mech. **44**, 479–504 (2012).
19. J. Arnqvist, H. Bergrstrom, and C. Nappo, "Examination of the mechanism behind observed canopy waves," Agr. Forest. Meteorol. **218-219**, 196–203 (2016).
20. B. B. Bailey and R. Stoll, "The creation and evolution of coherent structures in plant canopy flows and the role in turbulent transport," J. Fluid Mech. **789**, 425–460 (2016).
21. E. G. Patton, T. W. Horst, P. P. Sullivan, D. H. Lenschow, S. P. Oncley, W. O. J. Brown, S. P. Burns, A. B. Guenther, A. Held, T. Karl, S. D. Mayor, L. V. Rizzo, S. M. Spuler, J. Sun, A. A. Turnipseed, E. J. Allwine, S. L. Edburg, B. K. Lamb, R. Avissar, R. Calhoun, J. Kleissl, W. J. Massman, K. T. P. U, and J. C. Weil, "The Canopy Horizontal Array Turbulence Study (CHATS)," Bull. Amer. Meteor. Soc. **92**, 593–611 (2011).
22. S. D. Mayor and S. M. Spuler, "Raman-shifted Eye-safe Aerosol Lidar," Appl. Optics **43**, 3915–3924 (2004).
23. S. M. Spuler and S. D. Mayor, "Scanning eye-safe elastic backscatter lidar at 1.54 microns," J. Atmos. Ocean. Technol. **22**, 696–703 (2005).
24. S. D. Mayor, S. M. Spuler, B. M. Morley, and E. Loew, "Polarization lidar at 1.54-microns and observations of plumes from aerosol generators," Opt. Eng. **46**, DOI: 10.1117/12.781,902 (2007).
25. E. R. Jachens and S. D. Mayor, "Lidar observations of fine-scale atmospheric gravity waves in the nocturnal boundary layer above an orchard canopy," in "26th International Laser Radar Conference," (Porto Heli, Greece, 2012).